Filipkovskii. 2017. *Int. J. Vehicle Structures & Systems*, 9(5), 288-295
ISSN: 0975-3060 (Print), 0975-3540 (Online)
doi: 10.4273/ijvss.9.5.05

International Journal of Vehicle Structures & Systems
Available online at www.maftree.org/eja

Joint Effect of Imbalance and Supports Vibration on the Rotor Nonlinear Oscillations of Aircraft Device

Sergey V. Filipkovskii

Theoretical Mechanics and Hydraulics Dept., Kharkov National Automobile and Highway University, Ukraine
Rocket Structural Design and Engg. Dept., National Aerospace University, Kharkov Aviation Institute, Ukraine
Email: filipkovskiisv@gmail.com

ABSTRACT:

In many devices and aggregates of aircrafts and other vehicles rotors are both sources of vibration and they are subjected to vibrational load from their supports. In this case, the disturbance load has a component with a frequency which is not a multiple with respect to the rotor speed. Here the method of analysis of forced oscillations of a rigid rotor on angular contact bearings with axial preload has been developed. The frequency responses of the system as well as orbits of spindle centers and Poincaré maps with the joint action of imbalance and supports vibration have been obtained. When the rotor rotational speed and the frequency of supports vibration are of the same order, the resonance and super-resonance oscillations in the main modes are realized. The dependence of resonance modes on the angle of contact of ball-bearings has been studied. This work is intended to improve the numerical analysis of the dynamics and design of structures in the aerospace industry and transport engineering.

KEYWORDS:

Rotor; Angular contact ball bearing; Supports vibration; Imbalance; Nonlinear oscillations

CITATION:

S.V. Filipkovskii. 2017. Joint Effect of Imbalance and Supports Vibration on the Rotor Nonlinear Oscillations of Aircraft Device, *Int. J. Vehicle Structures & Systems*, 9(5), 288-295. doi:10.4273/ijvss.9.5.05.

NOMENCLATURE:

a	Eccentricity of the disc
$\mathbf{A}_{II}(\omega,t)$	Vector of the supports vibration accelerations
$A_{IIx1} - A_{IIz}$	Amplitudes of vibration accelerations
C	Damping coefficient
$\mathbf{C}$	Damping matrix
d	Shaft diameter
d_B	Ball diameter
E	Young modulus
$\mathbf{f}$	Dimensionless nonlinear vector function
$\mathbf{F}$	Dimensionless nonlinear vector function
f_ω	Frequency of support vibration
f_Ω	Frequency of the shaft rotation
$\mathbf{G}$	Gyroscopic matrix
I_0 and I_1	Polar and diametrical moments of inertia of the disk
I_{C0}	Central moment of the shaft inertia relative to the axis z
I_{C1}	Central moment of the shaft inertia relative to the axes *x, y*
$\mathbf{K}(\mathbf{X})$	Vector function of components of elastic reactions of the bearing
l	Shaft length
$\mathbf{M}$	Mass matrix
m_0	Mass of the disk
m_S	Mass of the shaft
P_0	Force of axial preload
P_{xv}, P_{yv}, P_{zv}	Components of elastic reactions of the bearing along the coordinate axes
$\mathbf{Q}(t)$	The right-hand part vector
$\mathbf{Q}_D(\Omega,t)$	Vector of forces due to the disk imbalance
$\mathbf{Q}_{II}(\omega,t)$	Vector of kinematic excitation of oscillations
R_1	Inner race radius
R_2	Outer race radius
R_K	Groove radius
t	Time
T	Dimensionless period
$\mathbf{U}$	Vector of dimensionless generalized coordinates
u_x, u_y, u_z	Movements of the shaft sections in the directions of the coordinate axes
$\mathbf{V}$	Vector of dimensionless generalized velocities
$\mathbf{X}$	Vector of generalized coordinates
x, y, z	Cartesian coordinate set
x_i, y_i, z_i	Movements of the center of the inner ring relative to the center of the outer ring
$x_1(t), y_1(t)$	Generalized coordinates of radial movements of spindle *A*
$x_2(t)$, $y_2(t)$	Generalized coordinates of radial movements of spindle *B*
x_A, y_A	Dimensionless coordinates of radial movements of spindle *A*
x_B, y_B	Dimensionless coordinates of radial movements of spindle *B*
$\mathbf{Y}$	Vector of dimensionless phase coordinates
$\mathbf{Y}_0$	$=\mathbf{Y}(0)$
$\mathbf{Y}_T$	$=\mathbf{Y}(T)$
z_0	axial displacement of the inner ring relative to the outer ring due to force P_0
$z_1(t)$	generalized coordinate of axial movements of shaft
z_A	Dimensionless coordinate of axial movements of shaft

α	Contact angle
β_ν	Angular location of ν^{th} ball
ζ	Coordinate of the shaft section along the axis *z*
ζ_D	Disk coordinate along the axis *z*.
ι	$=\overline{1,2}$ Indexes of the spindles
$\lambda = \xi \pm i\psi$	Multipliers of monodromy matrix
μ	Poisson's ratio
ν	Index of ball
N_B	Number of balls
τ	Dimensionless time
T_D	Kinetic energy of the disk
T_S	Kinetic energy of the shaft
Φ	Dissipation function
ω	Angular frequency of the vibration of supports
$\overline{\omega}$	Dimensionless angular frequency of the vibration of supports
$\overline{\omega}_1 - \overline{\omega}_5$	Dimensionless angular frequencies of resonance oscillations
Ω	Angular velocity of the rotor
Π	Potential energy of the system deformation

1. Introduction

Analysis of transverse oscillations of rotors is an important part of the design of many machines and mechanisms [1]. Non-linear analysis allows predict resonances and unstable modes of oscillations that can have a significant impact on the operation of the machine, but cannot be detected by analysis of linear models. Nonlinearity is noticeably exhibited at high loads. The great dynamic loads are typical for the rotors of aircrafts and other vehicles. Such rotors are often loaded with longitudinal loads; in this case they are mounted on angular contact ball bearings. The nonlinear analysis at the stage of design allows to predict resonances and unstable modes of oscillations which can lead to damage of a structure. The nonlinearity of the rotor ball-bearings system is caused both by nonlinear contact stresses and clearance between the balls and races [2]. Most publications consider nonlinear oscillations of the rotor on ball-bearings which have a clearance between balls and races.

Tiwari et al. [3] investigated the impact of the inner radial clearance and the effect of the variable rigidity on period-doubling bifurcations and the intermittency which led to chaos. Young et al. [4] investigated the parametric instability of the shaft on ball-bearings under the action of the variable of the axial force. Harsha [5, 6, 7] analyzed the effect of the inner radial clearance, waviness of races surface and rotational speed of a rigid rotor on periodic, subharmonic, chaotic oscillations and Hopf bifurcation. The results of numerical integration are presented in the form of Poincaré maps and frequency spectra. Xuening et al. [8] showed that the unbalanced force can make the bearing stiffness vary periodically and that the parametric excitation from the time-varying bearing stiffness can cause instability and severe vibration under certain operation conditions. Tomovic et al. [9] described the model of the rigid rotor vibration which helped to analyze the influence of the size of the inner radial clearance and the number of rolling elements in the bearing on parametric oscillations of the rigid rotor.

Yadav et al. [10] investigated the dynamic behaviour of a high-speed unbalanced rotor on the ball-bearings with inner radial clearance; it is shown that the quasiperiodic behaviour is the way to chaos. Rotors of many units must be protected from the blows and prohibitive displacements which can appear as a result of closing the clearances between balls and races of bearings. Such rotors are mounted on the angular contact bearings with axial preload. Bai et al. [11] investigated numerically and experimentally the transverse oscillations of the rotor on angular contact bearings with axial preload caused by the disk imbalance and showed their dependence on nonlinear contact forces. Dependences of the rotor stability and bifurcations on the magnitude of force of ball-bearings axial preload and rotational speed were investigated in the work [12]. Cui et al. [13] analyzed impacts of the initial contact angles, imbalance, a damping factor, axial preload, bending moments, factors of stiffness and rotating speed on stability and bifurcations of the rotor-bearing system.

Filipkovskii and Avramov [14] investigated free oscillations of the rotor on angular contact ball-bearings with axial preload by the method of nonlinear normal modes and obtained the backbone curves at different contact angles of the bearing. Aini et al. [15] investigated the effect of the frictional force and combined radial and axial forces on frequency responses of the rigid spindle on bearings with the axial preload. Alfares et al. [16] considered the effect of the bearing axial preload on the vibration characteristics of the grinding machine spindle and determined an optimum axial preload. The rotor oscillations can be caused by vibrations of bearings. Their causes are the presence in the bearing of a set of solids moving with different angular velocities, the deflection of the surfaces of balls and races from the ideal shape, the imbalance of the rings and the cage, the misalignments of a rotary machine assembling, defects appearing during operation [2, 17].

Many units of aircraft and sea craft, for example gyroscopic instruments, fans, centrifugal compressors, cooling turbines of planes work in conditions of vibration which is transferred by the airframe or the hull even if vibration insulation is provided. As opposed to excitation which is caused by bearing imperfection such disturbance load has a component with a frequency not a multiple of the rotor speed. The effect of the support vibration on the forced oscillations of a rotor has not been investigated sufficiently. If the range of a rotor rotational speed and the range of frequency of support vibration overlap, there will be beats of the exciting load which can lead to series of new resonances and transient regimes. The aim of this work is to research resonance oscillations of the rotor on angular contact bearings with preload, caused by the simultaneous action of imbalance and vibration of supports. At various stages of design of aerospace prototype models there is a need to change some parameters with preserving the general arrangement and sizes.

Therefore it seems natural to vary ball-bearing stiffness with the given sizes. The ball-bearing stiffness

can be varied by changing the contact angle. The standard provides angular contact bearings with the contact angles equal to 12°, 15°, 26°, 36° and 40°. It is therefore interesting to study the dependence of the resonance modes on the contact angle of the bearing.

2. Analytical model

The system of the rotor on the bearings consists of a shaft with a disk fixed eccentrically relative to supports (see Fig. 1). The designation and the conditions of operation of units in which axial preload of ball bearings is used, assume that the relationship of the length and diameter of the shaft provides the stiffness of the shaft by an order greater than that of bearings. Therefore, the shaft is considered to be a non-deformable body, and the degrees of freedom are the spindles movement relative to the bearing outer rings.

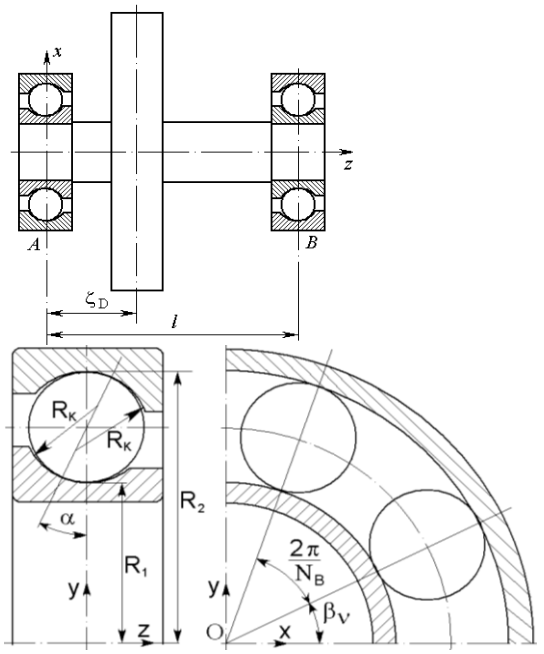

Fig. 1: Diagrams of the rotor and the ball bearing

Components of elastic reactions of the bearing along the coordinate axes x, y, z were derived in work [14].

$$P_{x\iota} = K\sum_{\nu=1}^{N_B} S_\iota^{3/2}\cos\alpha\cos\beta_\nu,\ P_{y\iota} = K\sum_{\nu=1}^{N_B} S_\iota^{3/2}\cos\alpha\sin\beta_\nu$$

$$P_{z\iota} = K\sum_{\nu=1}^{N_B} S_\iota^{3/2}\sin\alpha \qquad (1)$$

$$K = (3P_0/2N_B)z_0^{-3/2}\sin^{-5/2}\alpha;$$

$$S_{\nu,\iota} = x_\iota\cos\alpha\cos\beta_\nu + y_\iota\cos\alpha\sin\beta_\nu + (z_\iota + z_0)\sin\alpha$$

Where x_ι, y_ι, z_ι are the movements of the center of the inner ring relative to the center of the outer ring; $\iota = \overline{1,2}$ are the indexes of the spindles; angles α and β_ν are shown in Fig. 1(b); ν and N_B are the index and the number of balls; P_0 is the force of axial preload, z_0 is the axial displacement of the inner ring relative to the outer ring due to force P_0; angles α and β_ν are also shown in Fig. 1(b). Displacements x_ι, y_ι are small in comparison with the shaft length, therefore the rotor rotations around axes x, y can be neglected.

3. Equations of motion

The movements u_x, u_y of the shaft sections in the directions of the coordinate axes x, y are written as follows:

$$u_x(\zeta,t) = x_1(t)\frac{l-\zeta}{l} + x_2(t)\frac{\zeta}{l},$$

$$u_y(\zeta,t) = y_1(t)\frac{l-\zeta}{l} + y_2(t)\frac{\zeta}{l}, \qquad (2)$$

where l is the shaft length; ζ is the coordinate of the shaft section along the axis z; $x_1(t)$, $x_2(t)$, $y_1(t)$, $y_2(t)$ are the generalized coordinates of radial movements of spindles; t is the time. The inner rings of the ball bearings perform both radial and axial oscillations relative to the outer rings. Since the movements are small compared to the shaft length, oscillations of the rotor along the coordinate axis z can be described by one generalized coordinate $u_z = z_1(t)$. To generate the Eqns. of the motion we can use the Lagrange Eqns. On our assumption, the expression of the kinetic energy of the shaft T_S as a function of generalized coordinates will be as follows, Eqn. (3):

$$\begin{aligned} T_s = {} & \frac{I_{C1}}{2}\left(\frac{\dot y_1 - \dot y_2}{l}\right)^2 + \frac{I_{C1}}{2}\left(\frac{\dot x_2 - \dot x_1}{l}\right)^2 + \frac{I_{C0}}{2}\Omega^2 \\ & + I_{C0}\Omega\frac{(\dot y_1 - \dot y_2)(x_2 - x_1)}{l^2} \\ & + \frac{m_S}{2}\left(\frac{\dot x_1 + \dot x_2}{2}\right)^2 + \frac{m_S}{2}\left(\frac{\dot y_1 + \dot y_2}{2}\right)^2 \\ & + \frac{m_S}{2}\dot z_1^2 \end{aligned}$$

Where m_S is the mass of the shaft; I_{C0} and I_{C1} are the central moments of the shaft inertia relative to the axis of rotation and transverse axes; Ω is an angular velocity of the rotor. The kinetic energy of the disk T_D which is fixed on the shaft with the eccentricity α as a function of generalized coordinates will be as follows, Eqn. (4):

$$\begin{aligned} T_D = {} & \frac{I_1}{2}\left(\frac{\dot y_1 - \dot y_2}{l}\right)^2 + \frac{I_1}{2}\left(\frac{\dot x_2 - \dot x_1}{l}\right)^2 + \frac{I_0}{2}\Omega^2 \\ & + I_0\Omega\frac{(\dot y_1 - \dot y_2)(x_2 - x_1)}{l^2} \\ & + \frac{m_0}{2}\left[\dot x_1\left(1 - \frac{\zeta_D}{l}\right) + \dot x_2\frac{\zeta_D}{l} \right. \\ & \left. - a\Omega\sin\Omega t\right]^2 \\ & + \frac{m_0}{2}\left[\dot y_1\left(1 - \frac{\zeta_D}{l}\right) + \dot y_2\frac{\zeta_D}{l} \right. \\ & \left. + a\Omega\cos\Omega t\right]^2 + \frac{m_0}{2}\dot z_1^2 \end{aligned}$$

Where m_0 is the mass of the disk; I_0 and I_1 are the polar and diametrical moments of inertia of the disk, respectively; ζ_D is the disk coordinate along the axis z.

From the assumption that the shaft is non-deformable, it follows that the potential energy of the system deformation is represented only by the energy of deformation of bearings $\Pi = \Pi(x_1, y_1, x_2, y_2, z_1)$. The

derivatives of the potential energy in the generalized coordinates are the right sides of Eqns. (1). Damping is usually determined on the basis of experiments and is described by the model of viscous friction [15]. In this case, the Rayleigh dissipation function Φ has the following form:

$$\varphi = \mathrm{C}(\dot{x}_1^2 + \dot{y}_1^2 + \dot{x}_2^2 + \dot{y}_2^2 + \dot{z}_1^2)/2 \quad (5)$$

Where C is a damping coefficient. Using Eqn. (1) and Eqns. (3) to (5) we can obtain the equations of oscillations in the matrix form,

$$\mathrm{M}\ddot{\mathrm{X}} + \mathrm{G}\dot{\mathrm{X}} + \mathrm{C}\dot{\mathrm{X}} + \mathrm{K(X)} = \mathrm{Q(t)} \quad (6)$$

Where M is the mass matrix; G is the gyroscopic matrix; C is the damping matrix; K(X) is the vector function with nonlinear functions of Eqns. (1) as its components, X is the vector of the generalized coordinates, Q(t) is the right-hand part vector. The oscillations are excited by the joint action of the disk imbalance and the supports vibration, therefore:

$$Q(t) = Q_D(\Omega, t) + Q_{\Pi}(\omega, t),$$

Where $Q_D(\Omega, t)$ is the vector of forces due to the disk imbalance, $Q_{\Pi}(\omega, t)$ is the vector of oscillations kinematic excitation, ω is the angular frequency of the vibration of supports. The first vector

$$Q_D(\Omega, t) =$$
$$A_D\left[l_A \cos\Omega t \quad l_A \sin\Omega t \quad l_B \cos\Omega t \quad l_B \sin\Omega t \quad 0\right]^{\mathrm{T}},$$

Where $A_D = m_0 a\Omega^2$; $l_A = (1 - \zeta_D/l)$; $l_B = \zeta_D/l$ is obtained as a result of derivation of Eqn. (4). The second vector should be written down as follows [18]:

$$Q_{\Pi}(\omega, t) = -M \cdot A_{\Pi}(\omega, t),$$

Where $A_{\Pi}(\omega, t)$ is a vector of vibration accelerations of the supports,

$$A_{\Pi}(\omega t) = \left[A_{\Pi x1} \quad A_{\Pi y1} \quad A_{\Pi x2} \quad A_{\Pi y2} \quad A_{\Pi z}\right]^{\mathrm{T}} \sin\omega t,$$

Where $A_{\Pi x1}$, $A_{\Pi z}$ are the amplitudes of vibration accelerations.

4. Analysis of forced oscillations by continuation method

To study periodic solutions of the Eqn. (5), we build a frequency ω response of peak-to-peak displacements; frequency Ω is considered to be fixed. Let us define the dimensionless parameters as follows: $x_A = x_1/z_0$, $y_A = y_1/z_0$, $x_B = x_2/z_0$, $y_B = y_2/z_0$, $z_A = z_1/z_0$, $\bar{\omega} = \omega/\omega_1$, $\tau = t \cdot \omega_1$, where ω_1 is the main resonance frequency of the linearized system when $\alpha = 15^{\circ}$. The Eqn. (5) can be written in the form of a nonlinear vector function f:

$$\ddot{\mathrm{U}} = f(\mathrm{U}, \dot{\mathrm{U}}, \bar{\omega}, \tau) \quad (7)$$

Where $U = \left[x_A \quad y_A \quad x_B \quad y_B \quad z_A\right]^{\mathrm{T}}$ is the vector of dimensionless generalized coordinates. Having denoted $V = \dot{U}$, we rewrite Eqn. (7) in the form of the system of differential Eqns. of the first-order,

$$\dot{\mathrm{Y}} = F(\mathrm{Y}, \bar{\omega}, \tau) \quad (8)$$

Where F is a vector function, $Y = \{V \quad U\}^T$. The condition of periodicity of the solutions of Eqn. (8) can be written like that:

$$Y(0) = Y(T) \quad (9)$$

Where T is the period. If we consider vectors $Y_0 = Y(0)$ and $Y_T = Y(T)$ which determine the state of the system of Eqn. (8) at the moment of time $\tau = 0$ and $\tau = T$, the Cauchy problem (8) with boundary conditions (9) can be transformed into the solution of the implicit Eqn.

$$\left[Y(Y_0)\right]_T = Y_0 \quad (10)$$

To construct the frequency response we analyze Eqns. (10) by the continuation method [19]. At every stage of calculations we receive the monodromy matrix, its multipliers $\lambda = \xi \pm i\psi$ determine stability and nature of bifurcations of the periodic solution of the equation [20].

5. Results and discussions

Oscillations of a non-deformable rotor with one disk are considered. The rotor parameters are as follows: l = 0.5m, Zd = 0.125m, diameter of the shaft d = 0.025m, m_0 = 10kg, I_1 = 0.1kg·m^2, I_0 = 0.2kg·m^2. Rotational frequency $f_\Omega = \Omega/2\pi$ is taken to be close to the main resonance frequency of the rotor for each contact angle. Oscillations are excited by imbalance of the disk whose eccentricity is a = 0.008mm and by vibration of supports with the amplitudes of AΠx = 0, Aπy = 2g. Frequency of vibration $f_\omega = \omega/2\pi$ changes in the range from 20Hz to 2000Hz. The specific parameters of the bearing are as follows: outer race radius is R_2 = 27.5167mm; inner race radius is R_1 = 16.000mm; groove radius is RK = 5.930mm; ball diameter is dB = 11.510mm; NB = 7; Young modulus is E = 2.1·10^{11}Pa; Poisson's ratio is μ = 0.3. With such parameters $\omega_1 = 1250.78$ rad/s and $0.1 \le \bar{\omega} \le 10$.

5.1. Frequency response analysis

The areas of the main resonances of the frequency response caused by the joint action of imbalance and vibration of the supports at various contact angles are shown in Fig. 2. Lines 1, 2, 3, 4 and 5 correspond to contact angles α equal to 12°, 15°, 26°, 36° and 40°, respectively. The main resonances correspond to the vibration mode when the shaft spindles are located on the same side from the axis of symmetry of bearings, and during oscillations their centers move along the circular orbits in the direction of the shaft rotation, i.e. the shaft makes a direct precession. The bigger the angle is, the bigger the curvature of the race surface in the zone of contact is and, respectively, the lower rigidity of the zone of contact and frequency are. The frequency responses of the rotor-bearings system with the contact angles α=12° and α=15° are shown in Figs. 3, 4, respectively. With the joint action of imbalance and vibration of supports all modes of the rotor oscillations are exited. We denote the resonance frequencies in ascending order from $\bar{\omega}_1$ to $\bar{\omega}_5$. The rotor oscillations along the rotation axis have the lowest frequency $\bar{\omega}_1$. Resonance oscillations in the mode when shaft spindles are located on the opposite side from the axis of bearings

and the shaft makes a direct precession, have the highest frequency $\overline{\omega}_5$ and rather small peak-to-peak displacements.

Resonance oscillations in the mode when shaft spindles are located on the same side from the axis of bearings and the shaft makes a direct precession, have the middle frequency $\overline{\omega}_3$ and the biggest peak-to-peak displacements. Resonance oscillations have the low frequency $\overline{\omega}_2$ in the mode when shaft spindles are located on the same side from the axis of bearings and the shaft makes a retrograde precession, such oscillations are practically unnoted. In each mode also super-resonance oscillations which have frequencies related as integers are excited. Super-resonances have the most noticeable peak-to-peak displacements in the modes which correspond to frequencies $\overline{\omega}_3$ and $\overline{\omega}_5$. Super-resonances in the modes which correspond to frequency $\overline{\omega}_5$ are marked in Figs. 3, 4 $\overline{\omega}_5/2$, $\overline{\omega}_5/3$ etc. Their frequencies are related to the frequency of the main resonance as 1/2, 1/3 etc. In the Figs. 3, 4 super-resonances with lower frequencies corresponding to this mode are noticeable but their peak-to-peak displacements are small. Super-resonances in the mode when shaft spindles are located on the opposite sides from the bearings axis and the shaft makes a retrograde precession with the frequency $\overline{\omega}_4$ are practically un-noticed. Super-resonances in the modes which correspond to frequency $\overline{\omega}_3$ are marked in Figs. 3, 4 $\overline{\omega}_3/2$, $\overline{\omega}_3/3$, $\overline{\omega}_3/4$, $\overline{\omega}_3/5$ and their frequencies are related to the main resonance frequency as 1, 1/2, 1/3, 1/4, 1/5.

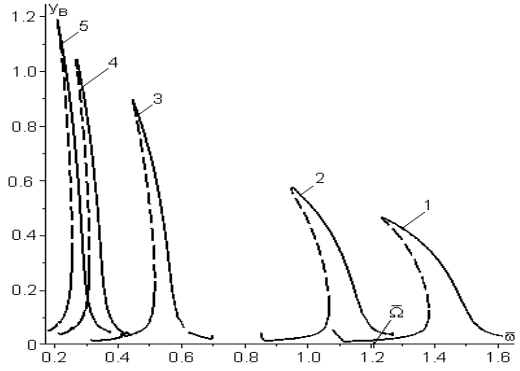

Fig. 2: The frequency response of the coordinate y_B under the action of imbalance and supports vibration

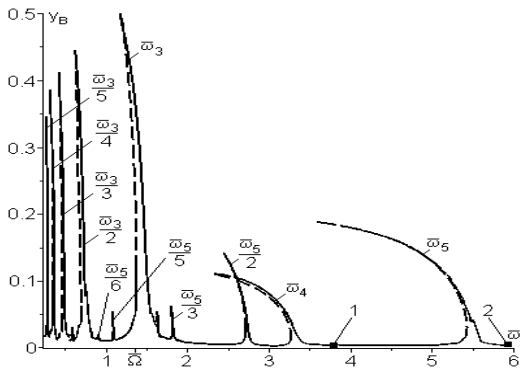

Fig. 3: The frequency response under the action of imbalance and supports vibration, α=12°

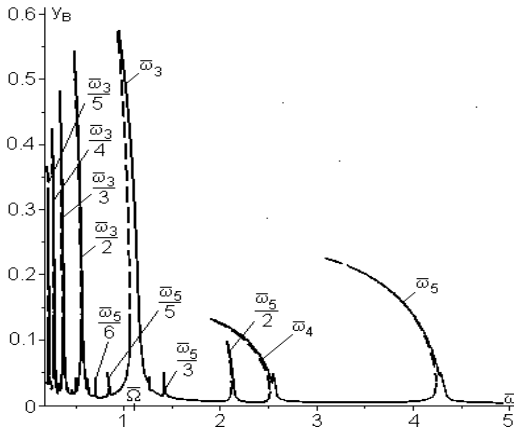

Fig. 4: The frequency response under the action of imbalance and supports vibration, α=15°

In Figs. 5-7 the frequency responses at contact angles 26°, 36° and 40° are shown. It is clearly seen that with increasing the contact angle the peak-to-peak displacements in modes which correspond to frequencies $\overline{\omega}_4$ & $\overline{\omega}_5$ decrease and the peak-to-peak displacements in the mode which corresponds to frequency $\overline{\omega}_3$ grow. On the left branches of all resonance peaks saddle-node bifurcations can be observed while on right branches one can observe Neimark-Sacker bifurcations. At the small contact angles the same bifurcations are observed to the right of the bases of resonance peaks as marked by points 1 & 2 in Fig. 3.

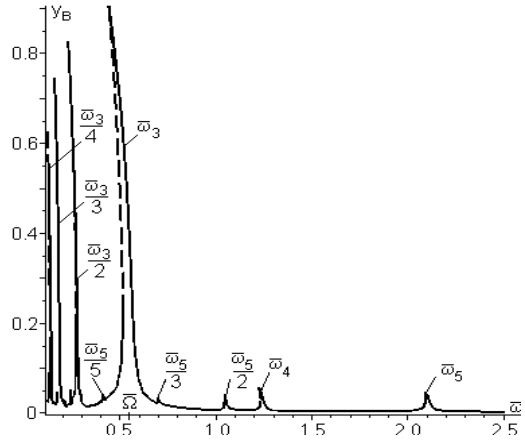

Fig. 5: The frequency response under the action of imbalance and supports vibration, α=26°

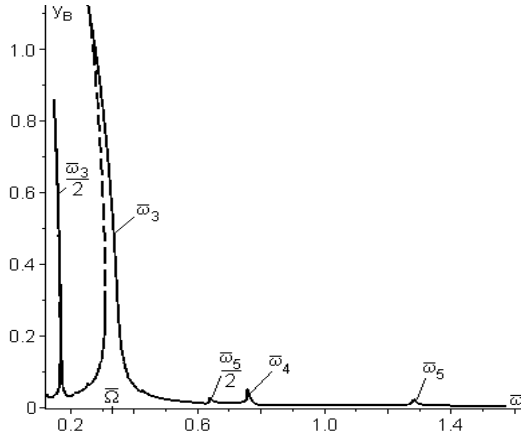

Fig. 6: The frequency response under the action of imbalance and supports vibration, α=36°

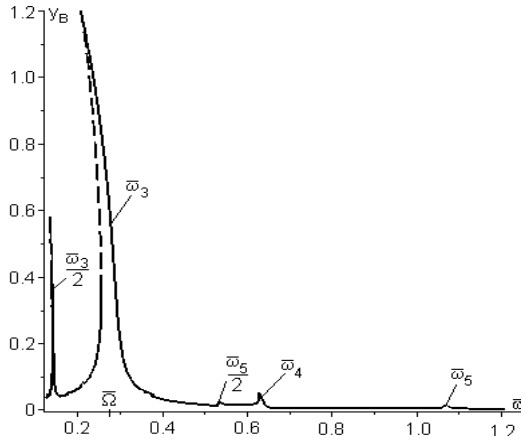

Fig. 7: The frequency response under the action of imbalance and supports vibration, α=40°

5.2. Stable oscillations analysis

Stable resonance oscillations of the rotor on ball-bearings with the angle of contact α=15 have been studied. Oscillations on the main resonance $\overline{\omega}_3$ have the biggest peak-to-peak displacements as is shown in Fig. 4. On this resonance peak the orbits of the spindles centers are close to circles, as is shown in Fig. 8. On super-resonances in the low-frequency range the peak-to-peak displacements of the oscillations is relatively small. Fig. 9 shows the orbit of the spindle B on the left branch of the super-resonance $\overline{\omega}_3/5$. The stable oscillations on the resonances in the mode that corresponds to frequency $\overline{\omega}_5$ have been studied. The peak-to-peak displacement of oscillations in this mode is smaller than that in the mode that corresponds to frequency $\overline{\omega}_3$, but nonlinearity is more noticeable.

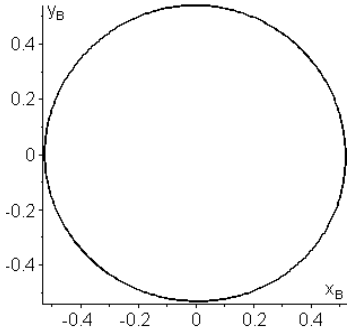

Fig. 8: Orbit of spindle B on the right branch of the resonance $\overline{\omega}_3$, $\overline{\omega}=0.9858$

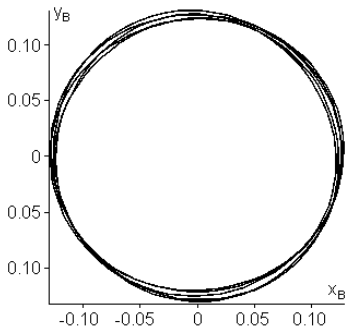

Fig. 9: Orbit of spindle B on the left branch of the super-resonance $\overline{\omega}_3/5$, $\overline{\omega}=0.2249$

In Fig. 10 the orbit of the spindle B near the point of bifurcation on the right branch of the resonance peak $\overline{\omega}_5$ is shown. Similar to those on the resonance $\overline{\omega}_3$ spindles orbits are close to circles but unlike the orbits on the resonance $\overline{\omega}_3$ the orbits of the spindle A have the bigger radii than the orbits of the spindle B. The orbits of the spindles on the left branch of the resonance peak $\overline{\omega}_5$ have a similar view. The orbits of the spindles on the super-resonances of this mode of the rotor oscillations have been studied. Fig. 11 shows the orbit of spindle B on the left branch of the super-resonance peak $\overline{\omega}_5/3$. The peak-to-peak displacement of the spindle B is small and the overlapping of the other oscillation mode becomes clearly explicit. For super-resonance frequencies for one period of oscillations the centers make so many loops, how many times the frequency is lower than the fundamental frequency for this mode.

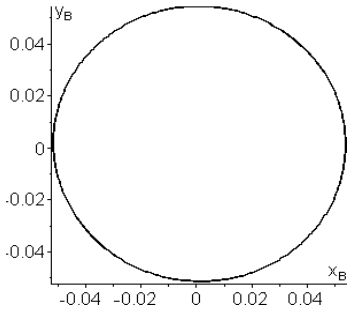

Fig. 10: Orbit of spindle B on the right branch of the resonance $\overline{\omega}_5$, $\overline{\omega}=4.2585$

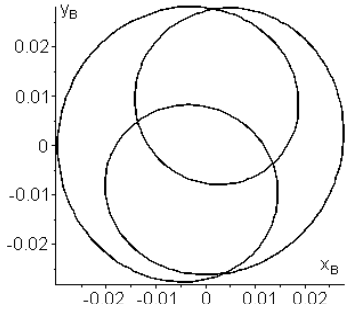

Fig. 11: Orbit of spindle B on the left branch of the super-resonance $\overline{\omega}_5/3$, $\overline{\omega}=1.4222$

5.3. Unstable oscillations analysis

The unstable oscillations of the rotor on the ball-bearings with the angle of contact α=15° have also been studied. On the left branches of resonance peaks the unstable modes of oscillations are observed for which the biggest multiplier of the monodromy matrix becomes the real number $\lambda_1>1$. That is, the saddle-node bifurcations occur in these points. On the right branches the unstable modes appear near the tops of the resonance peaks, modules of the biggest complex conjugate multipliers increase up to values $|\lambda_{1,2}|>1$ That is, Neimark-Sacker bifurcations in these points occur. For the analysis of the rotor dynamics in unstable modes we build by numerical integration the orbits of the spindles centers, generalized coordinates time responses and Poincaré maps. At first we investigate the unstable modes on the main resonances. In Fig. 12 the orbit of spindle B is shown for ten periods

at frequency $\overline{\omega} = 3.5932$ on the right branch of the resonance peak $\overline{\omega}_5$ (see Fig. 4).

In Fig. 13 the time response of the generalized coordinate y B for the same time is shown. Fig. 14 shows the Poincaré maps of spindle B oscillations in this mode. Here the biggest complex conjugate multipliers of the monodromy matrix are $\lambda_{1,2} = 0.89164 \pm 0.45715i$. The orbits of the spindles are close to circles whose radii change in time. From Figs. 12-14 we can see that the peak-to-peak displacements of oscillations remain restricted and there is a transition to beats. On the resonances $\overline{\omega}_4$ and $\overline{\omega}_3$ the same bifurcations and transition to beats can be observed. Then we investigate the unstable modes with big peak-to-peak displacements on super-resonances.

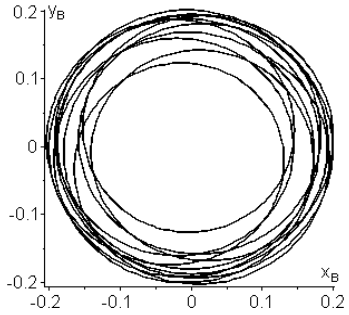

Fig. 12: Orbit of spindle B on the right branch of the resonance $\overline{\omega}_5$

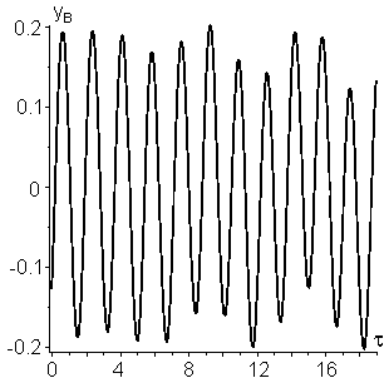

Fig. 13: Dependence y_B on time on the right branch of the resonance $\overline{\omega}_5$

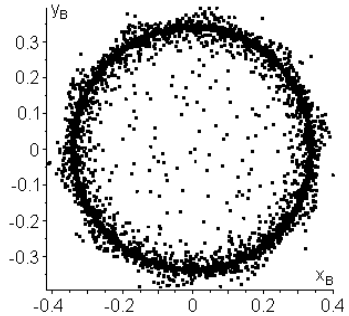

Fig. 14: Poincaré map of spindle B on the right branch of the resonance $\overline{\omega}_5$

In Fig. 15 the orbit of spindle B is shown for ten periods at frequency $\overline{\omega} = 0.3435$ in the area of bifurcation on the right branch near the top of the resonance peak $\overline{\omega}_3/3$. Here the complex-conjugate pair of the biggest multipliers of the monodromy matrix is $\lambda_{1,2} = 0.71570 \pm 0.72989i$. The orbits of the spindles look like the circles whose radii change in time considerably. Fig. 16 shows the time response of the generalized coordinate y_B on this super-resonance. Fig. 17 shows the Poincaré map of oscillations of spindle B in this mode. From Figs. 15-17 we can see that the peak-to-peak displacements of oscillations remain restricted and there is a transition to beats. The research proved that all other bifurcations also led to beats.

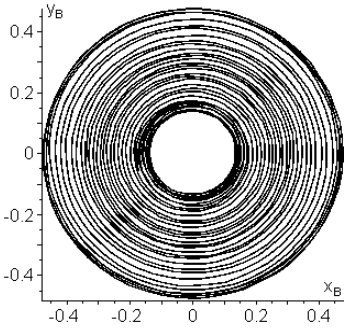

Fig. 15: Orbits of spindle B on the right branch of the super-resonance $\overline{\omega}_3/3$

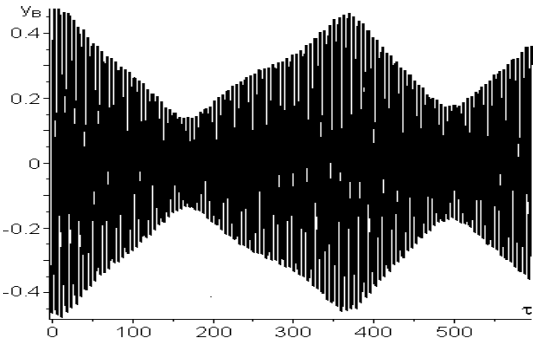

Fig. 16: Dependence y_B on time on the right branch of the super-resonance $\overline{\omega}_3/3$

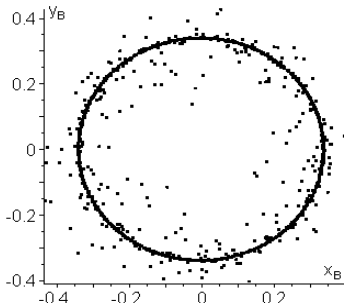

Fig. 17: Poincaré map of spindle B on the right branch of the super-resonance $\overline{\omega}_3/3$

6. Conclusions

The mathematical model of the rotor oscillations with five degrees of freedom on angular contact ball bearings with axial preload has been developed to investigate nonlinear oscillations of the rotor with a joint action of imbalance and vibrations of supports. As a result of application of the developed model it was established that with a joint action of imbalance and vibration of supports the oscillations in all modes are excited, both on the base resonance frequencies and on the super-resonance frequencies related as integers. With

increasing the contact angle the resonance frequencies decrease and the peak-to-peak displacements in the principal mode grow. At the small angles of contact there are frequency ranges without stable periodic modes of oscillations of the rotor on ball bearings. We can see the saddle-node bifurcations on the left branches of the resonance peaks and the Neimark-Sacker bifurcations on the right branches. In the unstable modes there is a transition to beats. Such behaviour of the system is explained by the fact that the frequency of support vibrations and the frequency of free oscillations are of the same order of magnitude. Overlapping of these oscillations generates beats of excitation which cause all considered resonances. The method and the results of this work can be used as a basis for improvement of numerical analysis of structural dynamics in the aerospace industry and transport engineering.

ACKNOWLEDGMENT:

This research is supported by two contracts with Antonov Company ("Development of a methodology and computer software for calculating the accelerations of the unit on shock absorbers under kinematic action for the rated cases of the product 77" and "Optimization of dynamic and strength properties of aircraft equipment suspended on shock absorbers").

REFERENCES:

[1] F.M. Dimentberg. 1961. *Flexural Vibrations of Rotating Shaft*, Butterworths, London, UK.

[2] T.A. Harris. 2001. *Rolling Bearing Analysis*, 4th Edition, John Wiley, New York, USA.

[3] M. Tiwari, K. Gupta and O. Prakash. 2000. Effect of radial internal clearance of a ball bearing on the dynamics of a balanced horizontal rotor, *J. Sound & Vibration*, 238(5), 723-756. https://doi.org/10.1006/jsvi.1999.3109.

[4] T.H. Young, T.N. Shiau and Z.H. Kuo. 2007. Dynamic stability of rotor-bearing systems subjected to random axial forces, *J. Sound & Vibration*, 305(3), 467-480. https://doi.org/10.1016/j.jsv.2007.04.016.

[5] S.P. Harsha. 2006. Nonlinear dynamic analysis of a high-speed rotor supported by rolling element bearings, *J. Sound & Vibration*, 290, 65-100. https://doi.org/10.1016/j.jsv.2005.03.008.

[6] S.P. Harsha. 2005. Nonlinear dynamic analysis of an unbalanced rotor supported by roller bearing, *Chaos, Solutions and Fractals*, 26(1), 47-66. https://doi.org/10.1016/j.chaos.2004.12.014.

[7] S.P. Harsha. 2005. Non-linear dynamic response of a balanced rotor supported on rolling element bearings, *Mech. Systems and Signal Processing*, 19, 551-578. https://doi.org/10.1016/j.ymssp.2004.04.002.

[8] Z. Xuening, Q. Han, Z. Peng and F. Chu. 2013. Stability analysis of a rotor-bearing system with time-varying bearing stiffness due to finite no. of balls and unbalanced force, *J. Sound & Vibration*, 332(25), 6768-6784. https://doi.org/10.1016/j.jsv.2013.08.002.

[9] R. Tomovic, V. Miltenovic, M. Banic and A. Miltenovic. 2010. Vibration response of rigid rotor in unloaded rolling element bearing, *Int. J. Mech. Sci.*, 52(9), 1176-1185. https://doi.org/10.1016/j.ijmecsci.2010.05.003.

[10] H.K. Yadav, S.H. Upadhyay and S.P. Harsha. 2013. Study of effect of unbalanced forces for high speed rotor, *Proc. Engg.*, 64, 593-602. https://doi.org/10.1016/j.proeng.2013.09.134.

[11] C. Bai, H. Zhang and Q. Xu. 2013. Subharmonic resonance of a symmetric ball bearing-rotor system, *Int. J. Non-Linear Mechanics*, 50, 1-10. https://doi.org/10.1016/j.ijnonlinmec.2012.11.002.

[12] C. Bai, H. Zhang and Q. Xu. 2008. Effects of axial preload of ball bearing on the nonlinear dynamic characteristics of a rotor-bearing system, *Nonlinear Dynamics*, 53, 173-190. https://doi.org/10.1007/s11071-007-9306-2.

[13] L. Cui and J. Zheng. 2014. Nonlinear vibration and stability analysis of a flexible rotor supported on angular contact ball bearings, *J. Vibration & Control*, 20, 1767-1782. https://doi.org/10.1177/1077546312474679.

[14] S.V. Filipkovskii and K.V. Avramov. 2013. Nonlinear free vibrations of multi-disk rotors on ball bearings, *Strength of Materials*, 45(3), 316-323. https://doi.org/10.1007/s11223-013-9461-2.

[15] R. Aini, H. Rahnejat and R. Gohar. 1990. A five degrees of freedom analysis of vibrations in precision spindles, *Int. J. Machine Tools & Manufacture*, 30(1), l-18. https://doi.org/10.1016/0890-6955(90)90037-J.

[16] M.A. Alfares and A.A. Elsharkawy. 2003. Effects of axial preloading of angular contact ball bearings on the dynamics of a grinding machine spindle system, *J. Materials Processing Tech.*, 136, 48-59. https://doi.org/10.1016/S0924-0136(02)00846-4.

[17] K. Ragulskis, A. Jurkauskas, V. Atstupėnas, A. Vitkutė and A. Kulvec. 1979. *Vibration of Bearings*, New Delhi, India.

[18] S.P. Timoshenko, D.H. Young and W. Weaver. 1974. *Vibration Problems in Engg.*, John Wiley, New York, USA.

[19] R. Seydel. 1997. Nonlinear computation, *Int. J. Bifurcation and Chaos*, 7, 2105-2126. https://doi.org/10.1142/S0218127497001564.

[20] S. Wiggins. 1990. *Introduction to Applied Non-Linear Dynamical Systems and Chaos*, New York, USA. https://doi.org/10.1007/978-1-4757-4067-7.